Theory of quantum-dot-based loss compensation of surface plasmon-polaritons for plasmonic signal processing

SY. SHAFIEI*, R. YADIPOUR, H. BAGHBAN
Faculty of Electrical and Computer Engineering, University of Tabriz, Tabriz, Iran

In this paper, a theoretical model has been developed to calculate the loss compensation of the surface plasmon-polariton (SPP) propagation loss in a plasmonic structure. Quantum dots (QDs) have been considered as the active medium and a multi-layer structure has been proposed for analyzing the SPP propagation loss. The multi-layer structure of QDs is composed of a quartz substrate, a 50-nm-thick gold film, and a thin layer of polymethylmethacrylate (PMMA) with embedded CdSe QDs. An optical pump is used to achieve SPP amplification. First, we develop a theoretical model taking into account the non-uniformity of the pump irradiance distribution. The pump distribution in the structure is calculated by the transfer matrix method. To calculate the signal propagating distribution, rate equations for QSs have been used in the gain layer structure. Finally, by considering the aspects and combination of all mentioned equations, we simulate the whole structure and sweep design parameters to achieve the best performance. A maximum SPP loss compensation of about 40% is observed in the presented structure. This study presents a feasible method to alleviate the high loss in plasmonic waveguides and the introduced model can be used to design plasmonic integrated circuits with loss values comparable with optical integrated circuits.

(Received April 20, 2023; accepted October 14, 2025)

Keywords: Plasmonic, Plasmonic amplifier, Quantum dot, Rate equation, Plasmonic laser

1. Introduction

Surface plasmon (SP) waveguide structures are at the center of attention for the next generation of photonic integrated circuits (PICs) due to their high field enhancement and the capability to break the diffraction limit [1]. However, the ohmic loss limitation which is inherent to all devices exploiting plasmonic features has propelled the research interests toward the development of integrated plasmonic devices with broadband loss compensation potential and the new generation of SP structures with modified loss characteristics such as hybrid plasmonic waveguides [2] or active devices with plasmonic amplification capability [3] have been advent. In situ loss compensation guarantees safe transport of information in PICs, while important features such as cascadability and scalability can be expected. These major motivations are also technologically crucial achievements that pave the way for dense plasmonic integrated circuits with low threshold power, high dynamic range, and room-temperature operation. High-quality wireless communication can be benefitted from low-loss subwavelength plasmonic channels [4]. Also, the possibility of signal amplification through optical field enhancement can yield plasmonic biosensors with enhanced sensitivity and selectivity [5]. In recent years, the promising prospect of plasmonic integrated circuits has renewed the enthusiasm toward all-optical logic gates as building blocks of information processing and photonic computing as well as optical storage. While all-optical logic gates have encountered considerable challenges during the past two decades mainly due to the lack of integration capability in scenarios based on fiber-optics logic gates or technologically complex demonstrations in proposals relying on active elements such as semiconductor optical amplifiers [6], plasmonic logic gates (PLGs) are anticipated to overcome the aforementioned challenges. PLGs have been introduced in different platforms including plasmonic slot waveguides [7], hybrid plasmonic waveguides [8], dielectric loaded waveguides [9], insulator-metal-insulator (IMI) waveguides [10], and plasmonic waveguides with nonlinear (Kerr-type) optical effects [11]. Meanwhile, a novel generation of plasmonic devices exploits the phase change materials (PCM) to reduce the optical loss and power consumption in plasmonic operations and increase the switching speed in plasmonic switches and logic gates [12].

Regardless of the structural diversity of PLGs, an efficient loss reduction plan with low power consumption, easy and low-cost demonstration method, and compatibility with the operation principles of plasmonic integrated circuits can considerably boost the performance merits of plasmonic logic gates. Using fluorescent molecules as the gain medium [13], nanobelt hybrid plasmonic waveguide with optical gain [14], quantum wells as active gain medium at telecommunication wavelengths [15], optically-pumped dye solution [16], and experimental demonstration of quantum dots (QDs) inside a polymer matrix [17] have provided long-range surface

plasmon propagation in recent studies. On the other hand, QDs with low nonradiative losses, high optical absorption and gain coefficients, low-cost and simple fabrication methods especially in the solution phase can be merged with different plasmonic structures [18],[19].

To the best of our knowledge, this is the first time that a detailed calculation the reveals the capacity of QD gain-assisted plasmonic waveguides for the design and fabrication of plasmonic logical dates has been developed.To prove the efficiency of the introduced model, signal propagation and operation characteristics of a XOR logic gate have also been investigated. The introduced all-optical design alleviates the structural complexity of electro-optic plasmonic structures (e.g. used in PCM plasmonic switches) and limited propagation length of passive hybrid waveguides.

2. Experimental

The proposed structure is composed of a quartz (SiO2) substrate, a 50 nm-thick gold film, a thin layer of polymethylmethacrylate (PMMA) with embedded CdSe QDs with a determined density of Nd, and optical pumping has been used to achieve SPP amplification as shown in Fig. 1.

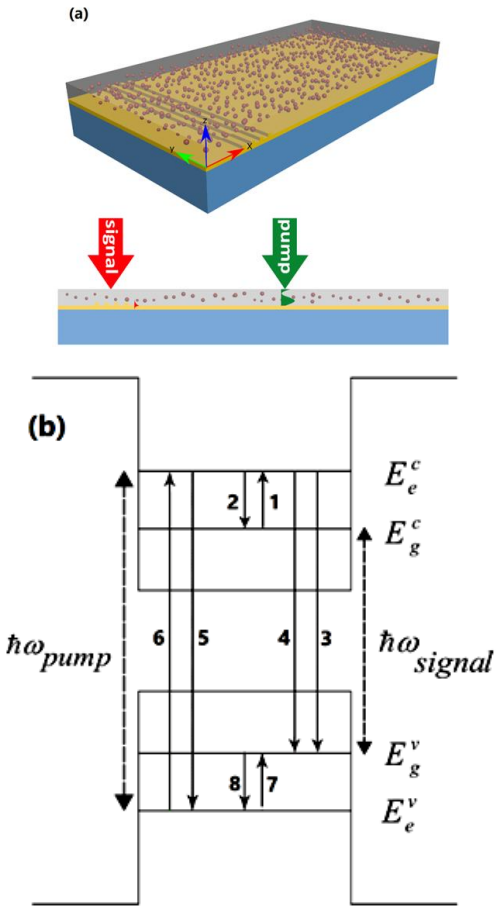

Fig. 1. (a) General geometry of the proposed structure and its cross-section, (b) Energy band structure of a CdSe QD based on a four-level energy approach (colour online)

As illustrated in Fig. 1 (a), the structure is excited by a monochromatic pump at λp = 532 nm and surface plasmon-polaritons (SPPs) are stimulated by the input signal of wavelength λs = 860 nm applied to the metal-dielectric interface. It is necessary to mention that close to the metallic surface the pump radiation is generally non-uniform because of CdSe QDs which leads to nonuniformity in pump distribution along the gain medium. On the other hand, optical loss in the propagation length of the signal decreases the length of SPP propagation. This effect can be estimated by the effective imaginary part of the dielectric permittivity of the PMMA layer, $\varepsilon^{"}$, using the following expression [18]:

$$\varepsilon^{"} = \frac{\sqrt{\varepsilon}\lambda}{2\pi} N\sigma_{abs} \tag{1}$$

Here, ε is the dielectric constant of PMMA, λ is the free-space wavelength, N is the concentration of QDs (inside the PMMA layer) which absorb at the wavelength λ, and σabs is the QD absorption cross-section. at λs = 860 nm has been considered [18]. Different approaches are available to obtain the reflection and transmission coefficient of the electromagnetic field when considering stratified media in terms of the electromagnetic theory of light. One of the most applicable approaches for multilayer structures is to employ matrix methods explained by Pettersson [19].

$$E_j(x) = \frac{S^{"}_{j11}.e^{-i\xi_j(d_j-x)} + S^{"}_{j21}.e^{+i\xi_j(d_j-x)}}{S^{'}_{j11}.S^{"}_{j11}.e^{-i\xi_j d_j} + S^{'}_{j12}.S^{"}_{j21}.e^{+i\xi_j d_j}} E_0^+ \tag{2}$$

where Ej(x) is the total electric field in an arbitrary plane in layer j at a distance x and is the incident plane wave. Equation (2) has been expressed in terms of the matrix elements of the partial system transfer matrices which all the coefficients have been explained in [19]. The pump irradiance distribution in each medium is computed as:

$$I_p(z) = \frac{\mathrm{Re}\eta(z)}{2|\eta(z)|^2}\left|E_p(z)\right|^2 \tag{3}$$

$$\eta(z) = \sqrt{\frac{\mu_0}{\varepsilon_0\varepsilon_r(z)}} \tag{4}$$

where η(z) is the characteristic impedance of the medium at the location z, εr(z) can be calculated using (1) and Ep(z), the pump electric-field distribution throughout the structure, can be computed by using the information reported in [20].

Coupled rate equations have been conducted for analyzing carrier dynamics and optical properties of the structure [21]. As claimed in prior studies, the rate equation model is a successful method in describing the pump–signal configuration. The coupled rate equations

approach (based on the transitions considered in Fig. 1(b)) used in this study is as follows:

$$\frac{dn_g^c}{dt} = -\frac{n_g^c}{\tau_{gr}}(1-f_g^v) + \frac{n_e^c}{\tau_{eg}^c}(1-f_g^c) - \frac{n_g^c}{\tau_{ge}^c}(1-f_e^c) - OCF \times L \times \frac{g_{signal} P_{signal}}{\hbar\omega_{signal}} \times (f_g^c(1-f_g^v)) \quad (5)$$

$$\frac{dn_e^c}{dt} = +\frac{n_g^c}{\tau_{ge}^c}(1-f_e^c) - \frac{n_e^c}{\tau_{eg}^c}(1-f_g^c) - \frac{n_e^c}{\tau_{er}}(1-f_e^v) + OCF \times L \times \frac{g_{pump} P_{pump}}{\hbar\omega_{pump}} \times (f_e^v - f_e^c) \quad (6)$$

$$\frac{dn_g^v}{dt} = +\frac{n_g^c}{\tau_{gr}}(1-f_g^v) + \frac{n_e^v}{\tau_{eg}^v}(1-f_g^v) - \frac{n_g^v}{\tau_{ge}^v}(1-f_e^v) + OCF \times L \times \frac{g_{signal} P_{signal}}{\hbar\omega_{signal}} \times (f_g^c(1-f_g^v)) \quad (7)$$

$$\frac{dn_e^v}{dt} = +\frac{n_g^v}{\tau_{ge}^v}(1-f_e^v) - \frac{n_e^v}{\tau_{eg}^v}(1-f_g^v) + \frac{n_e^c}{\tau_{er}}(1-f_e^v) + OCF \times L \times \frac{g_{pump} P_{pump}}{\hbar\omega_{pump}} \times (f_e^v - f_e^c) \quad (8)$$

where the optical power of the pump and the input probe signal are denoted by P_{pump}, P_{signal}. L and OCF are the waveguide length and the optical confinement factor, respectively. The terms n_g^c (n_g^v) and n_e^c (n_e^v) are the number of electrons in the ground state of the conduction band (valence band) and the number of electrons in the excited state of the conduction band (valence band), respectively. The corresponding carrier occupation probabilities are f_g^c (f_g^v) and f_e^c (f_e^v). The propagation equation of the input signal can be written as:

$$\frac{dP_{signal}}{dx} = (OCF \times g_{signal} \times (f_g^c(1-f_g^v)) - \alpha_{\text{int}}) P_{signal}(t,x) \quad (9)$$

where P_{signal} is the input probe signal power and α_{int} is the waveguide intrinsic loss. To solve the mentioned coupled equations (6-10), numerical analysis has been performed.

3. Results

We first examine how the pump is distributed in the introduced structure. For this purpose, by assuming constant structural materials, the results can be examined by making changes in metal and gain layer (PMMA) thicknesses as illustrated in Figs. 2 and 3, respectively. Fig. 2 exhibits the distribution of the normalized pump power extracted from various thicknesses of the gold layer for the fixed gain layer thickness of 200 nm. Increasing the thickness of the metal layer leads to higher pump power. The remarkable point of obtained curves is that the pump distribution gets saturated after a thickness of 70 nm. In fact, by increasing the thickness of the metal layer, the field is absorbed in the metal, and for higher thicknesses, the metal layer behaves like a semi-infinite metal film. Also, the pump distribution shows a sharp decrease in the metal region. After examining the metal layer thickness and obtaining the optimal value, the effect of PMMA layer thickness on the pump distribution in the structure is investigated. Assuming the constant metal layer thickness of 50 nm, the maximum values of the pump distribution for different thicknesses of the gain layer (1-500 nm) are plotted in Fig. 3.

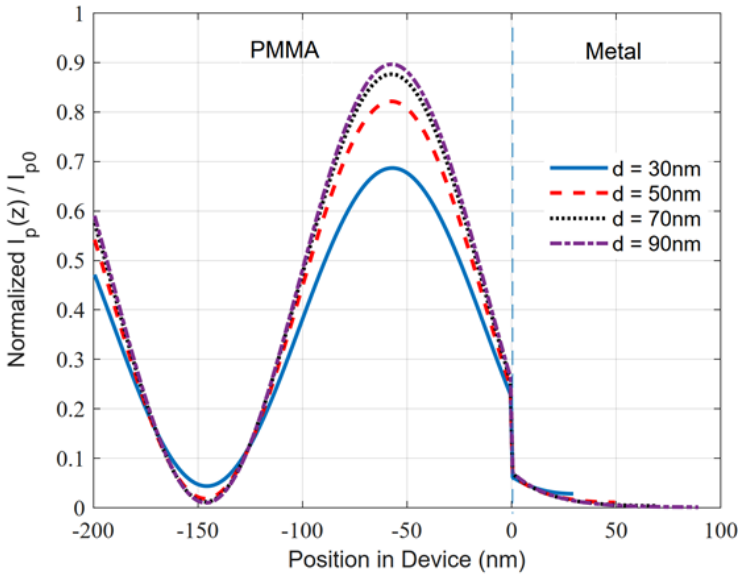

Fig. 2. Effect of metal thickness on the normalized pump distribution along the dielectric-metal growth direction (colour online)

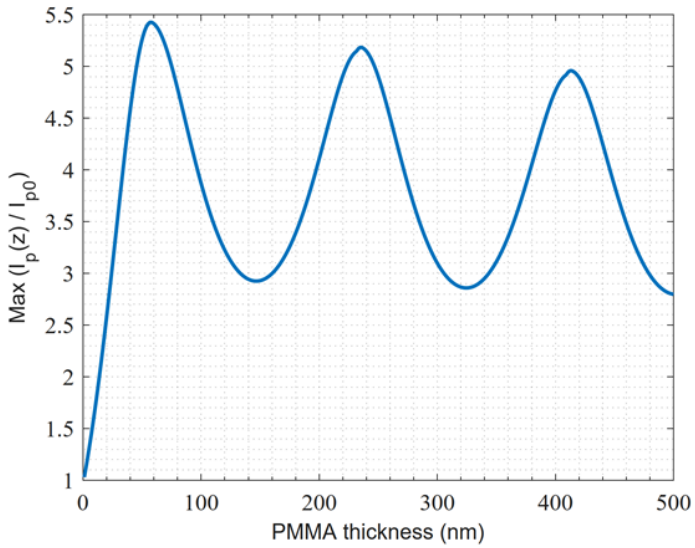

Fig. 3. Maximum pump distribution values for different PMMA layer thicknesses for a fixed metal layer thickness of 50 nm (colour online)

The effect of the density of QDs for different lengths of the proposed structure has been investigated and illustrated in Fig. 4. For this purpose, five different lengths have been considered for the structure, in which the power values of the output signals for different densities of QDs are shown. The input signal and pump powers are assumed to be 1mW and 20mW, respectively. The noteworthy point in the curves of Fig. 4 is that the maximum output power is achievable in a certain range of QD densities, which depends on the length of the structure and other structural parameters. As an instance, for a structure with a length of 50 µm, the maximum output power equals 0.555mW (Nd =3×1020 m-3). Additionally, as the length of the structure increases, the output signal decreases significantly due to the high propagation losses of the SPPs illustrated in Fig. 5. Figs. 6 and 7 report the effect of input pump and signal intensities on the performance of the proposed structure for two samples QD densities of Nd =3×1020 m-3 and Nd =3×1022 m-3, respectively. A structural length of L=10µm has been assumed in the later analysis as well. It is straightforward that for larger powers of the input signal, the percentage of SPP losses compensation is lower, which can be attributed to the increase in total power losses by increasing the intensity of the input signal. In other words, at higher powers of the input signal, the percentage of loss compensation is lower, which is due to the increased power losses by increasing the signal intensity compared to the pump signal.

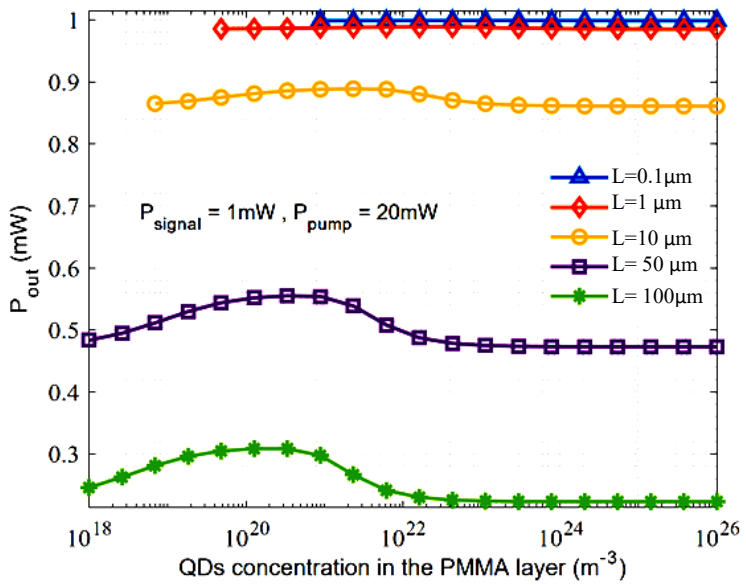

Fig. 4. Effect of the quantum dots density on the output signal power for different lengths of the structure (colour online)

The remarkable point of the curves plotted in Fig. 7 is that as the pump signal increases, an exponential decrease in the SPP losses can be observed. Indeed, the larger the amplitude of the pump signal applied to the structure, the higher the loss SPP compensation percentage. It is quite obvious that there is a significant decline in the dependence between the amount of losses compensation and the intensity of the input signal due to the rise in the number of quantum dots.

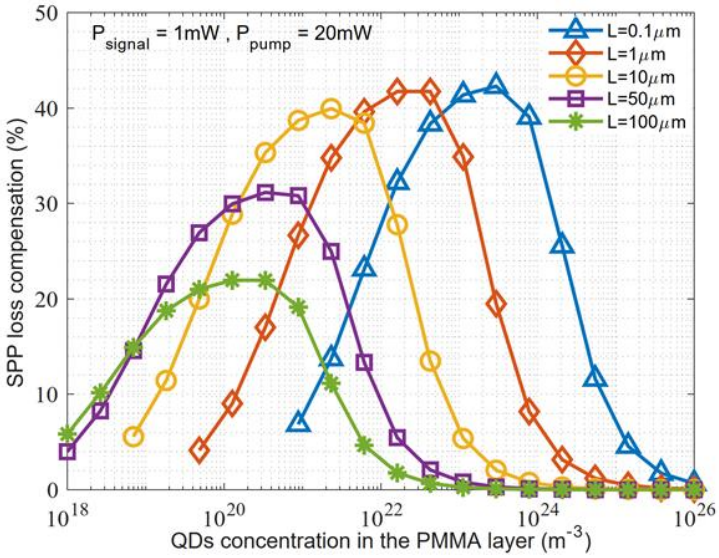

Fig. 5. Illustration of the percentage of compensation for SPP losses in terms of the density of quantum dots for various structure lengths (colour online)

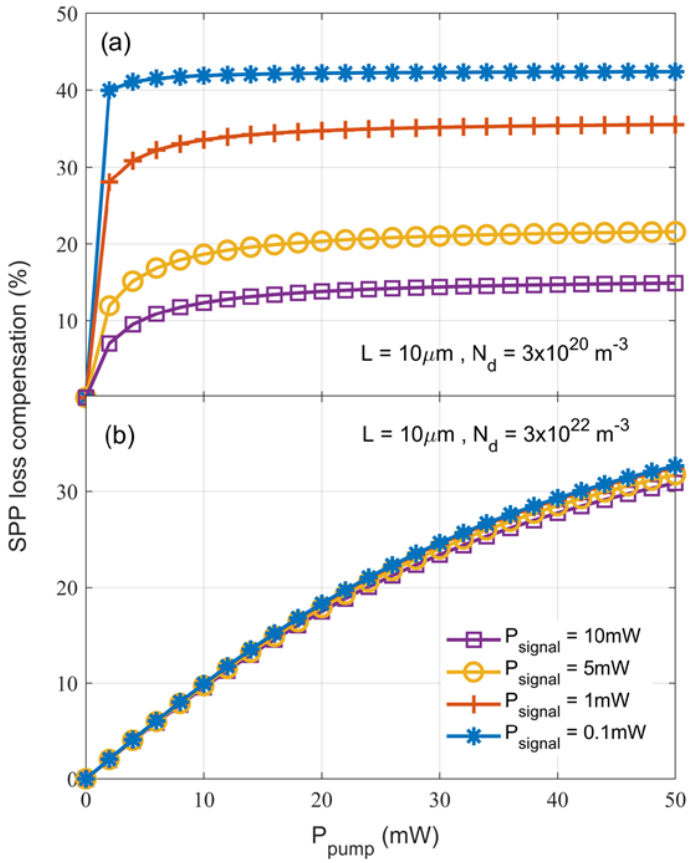

Fig. 6. a) Effect of pump signal intensity on the structure in terms of the percentage of compensation for SPP propagation losses. b) Effect of pump signal intensity on the structure in terms of the percentage of compensation for SPP propagation losses Nd =3×1022 m-3 and L=10 μm (colour online)

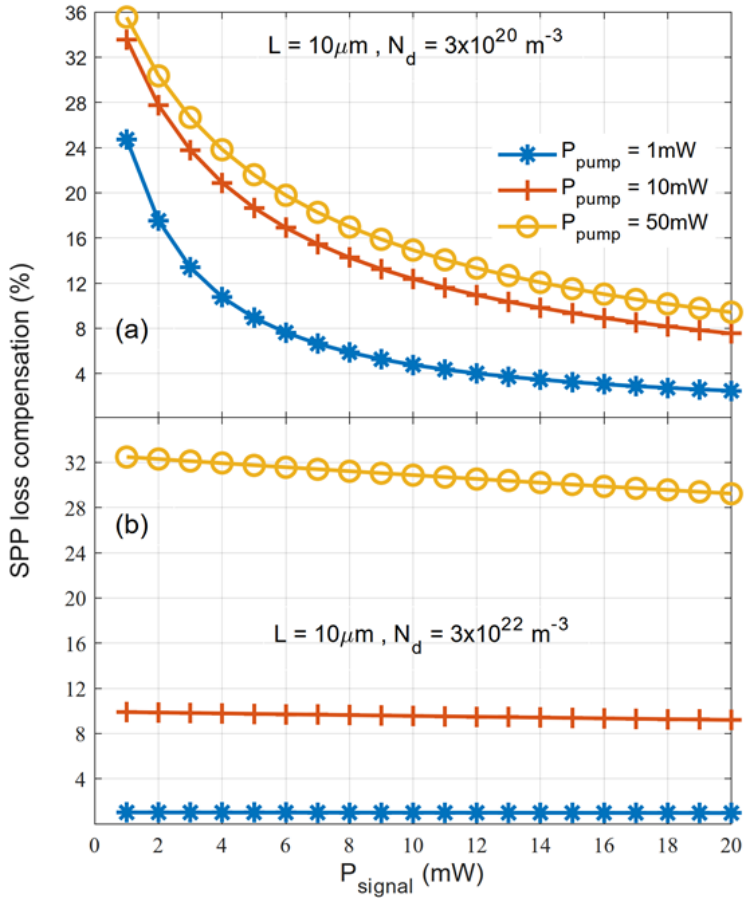

Fig. 7. (a) The proposed structure performance for various input signals in three different pump signals (Nd =3×1020 m-3); (b) The proposed structure performance for various input signals in three different pump signals (Nd =3×1022 m3) (colour online)

It was conluded that effect of loss reduction predicted in our results does not affect the operation of a logic gate but only the propagation length and the intensity of the output signal, Fig.8.

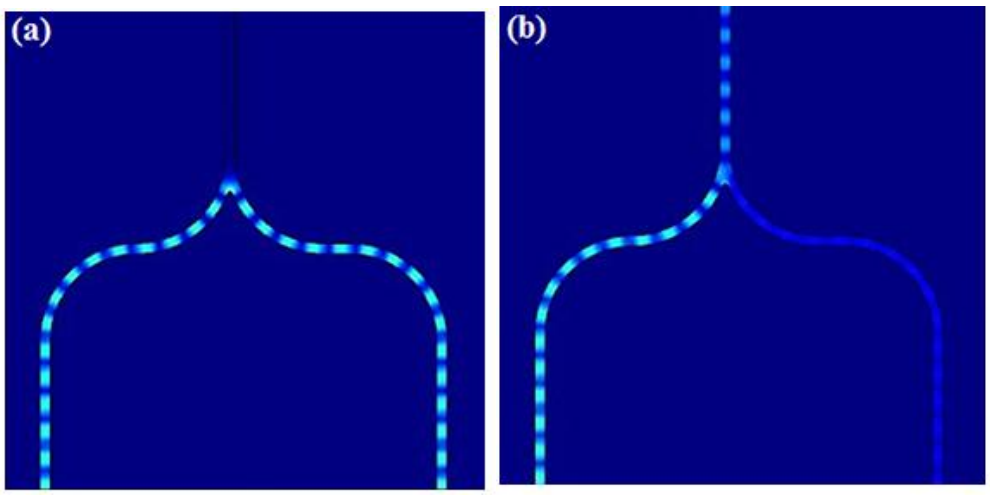

Fig. 8. (a) Operation of a plasmonic XOR logic gate with both inputs excited; (b) only one input is excited (colour online)

4. Discussion

All-optical logic gate devices in the nanoscale have attracted enormous attention in the past two decades because of their essential applications in the fields of optical computing and ultrahigh-speed information processing. These devises (OLG) have encountered considerable challenges during the past studies mainly due to the lack of integration capability in scenarios based on fiber-optics logic gates or technologically complex

demonstrations in proposals relying on active elements such as semiconductor optical amplifiers, plasmonic logic gates (PLGs) are anticipated to overcome the aforementioned challenges. PLGs have been introduced in different platforms including plasmonic slot waveguides, hybrid plasmonic waveguides, dielectric loaded waveguides, insulator-metal-insulator (IMI) waveguides, and plasmonic waveguides with nonlinear (Kerr-type) optical effects.

It is straightforward that SPPs lose their energy in the metal-dielectric interface due to electron scattering so there is a sizeable amount of loss propagation of SPPs at visible and near-infrared wavelengths. High propagation losses of the SPPs bring about a fundamental problem restricting utilizing all benefits of the SPPs. One effective way may be found in adding gain layer (polymethylmethacrylate) with embedded CdSe as quantum dots. To the best of our knowledge, there has been no previous report of the detailed model of coupled rate and propagation equations in which both time and spatial domains have been considered for describing the characteristics of an all optical modulator based on semiconductor quantum dots. Moreover, the capacity of QD gain-assisted plasmonic waveguides for the design and fabrication of plasmonic logical dates has been developed in this paper. In this case study a realistic theoretical model has been studied the generation and amplification of SPPs in two-dimensional planar metallic structures incorporating a QD gain medium taking into account the non-uniformity of the pump irradiance distribution.

5. Conclusion

In conclusion, this study presented a comprehensive theoretical framework for loss compensation in surface SPP waveguides using a multilayer plasmonic structure with QDs as the gain medium. By integrating a quartz substrate, gold film, and PMMA with embedded CdSe QDs, and employing optical pumping, the proposed design demonstrated up to 40% SPP loss compensation. The results highlight the importance of optimizing structural parameters such as the thickness of the metal and gain layers, as well as QD density, to maximize the structural performance. Numerical simulations revealed significant reductions in SPP propagation losses with increased pump intensity, enabling practical loss management in plasmonic devices. The study also explored the potential for all-optical logic gate operation, confirming that loss reduction does not impact logic gate function but enhances signal intensity and propagation length. These findings provide a viable pathway for designing efficient plasmonic integrated circuits with reduced loss and scalability comparable to optical integrated circuits, fostering advancements in photonic computing and high-speed data processing.

Acknowledgments

The authors thank the University of Tabriz for supporting this research.

References

[1] E. Cortés, A. O. Govorov, H. Misawa, K. A. Willets, The Journal of Chemical Physics **153**(010401), 1 (2020).
[2] D. A. Svintsov, A. V. Arsenin, D. Y. Fedyanin, Optics Express **23**(15), 19358 (2015).
[3] P. Berini, I. De Leon, Nature Photonics **6**, 16 (2012).
[4] H. Zhang, L. P. Zhang, P. H. He, J. Xu, C. Qian, F. J. Garcia-Vidal, T. J. Cui, Light: Science and Applications **9**, 113 (2020).
[5] H. Lu, R. Liu, P. Liu, W. Lin, Y. Huang, R. Xiao, Z. Li, J. Ma, W. Wang, J. Li, L. Sun, B. Guan, Optics Express **29**(9), 13937 (2021).
[6] A. Rostami, H. Baghban, R. Maram, Nanostructure semiconductor optical amplifiers: building blocks for all-optical processing, Springer, 2011.
[7] Z. Chen, J. Chen, Y. Li, D. Pan, W. Lu, Z. Hao, J. Xu, Q. Sun, IEEE Photonics Technology Letters **24**(16), 1366 (2012).
[8] L. Cui, L. Yu, Modern Physics Letters B **32**(2), 1850008 (2018).
[9] M. Ota, A. Sumimura, M. Fukuhara, Y. Ishii, M. Fukuda, Scientific Reports **6**, 24546 (2016).
[10] H. F. Fakhruldeen, T. S. Mansour, Advanced Electromagnetics **9**(1), 91 (2020).
[11] Y. Wu, Progress in Electromagnetics Research **170**, 79 (2021).
[12] R. Ghosh, A. Dhawan, Scientific Reports **11**, 18811 (2021).
[13] M. C. Gather, K. Meerholz, N. Danz,, K. Leosson, Nature Photonics **4**, 457 (2010).
[14] N. Liu, H. Wei, J. Li, Z. Wang, X. Tian, A. Pan, H. Xu, Scientific Reports **3**, 1967 (2013).
[15] M. Z. Alam, J. Meier, J. S. Aitchison, M. Mojahedi, Optics Express **15**(1), 176 (2007).
[16] J. Seidel, S. Grafström, L. Eng, Physical Review Letters **94**(17), 177401 (2005).
[17] P. M. Bolger, W. Dickson, A. V. Krasavin, L. Liebscher, S. G. Hickey, D. V. Skryabin, A. V. Zayats, Optics Letters **35**(8), 1197 (2010).
[18] I. P. Radko, M. G. Nielsen, O. Albrektsen, S. I. Bozhevolnyi, Optics Express **18**(18), 18633 (2010).
[19] L. A. Pettersson, L. S. Roman, O. Inganäs, Journal of Applied Physics **86**, 487 (1999).
[20] I. De Leon, P. Berini, Optics Express **17**(22), 20191 (2009).
[21] L. Balaghi, H. Baghban, M. Dolatyari, A. Rostami, IEEE Journal of Selected Topics in Quantum Electronics **19**(5), 1 (2013).

*Corresponding author: shafiei@tabrizu.ac.ir